Detection of Setting Time During Cement Hydration Using Multielectromagnetic Parameters of Patch Antenna Sensor

Zhuoran Yi, Songtao Xue, Liyu Xie, *Member, IEEE*, Guochun Wan, *Member, IEEE*, and Chunfeng Wan

***Abstract*— This article analyzes the feasibility of detecting the setting time of concrete paste using three electromagnetic parameters based on a novel patch antenna's return loss, bandwidth, and resonant frequency while embedded in cement paste. They also used two data fusion methods to reduce errors in predicting the setting time using the dielectric constant of cement paste. As the hydration of concrete increases, the moisture content of cement paste decreases, causing the dielectric constant of cement paste also to decrease. The radiation efficiency (represented by the return loss), bandwidth, and resonant frequency of the patch antenna shift due to variations in the dielectric constant of the covering material. The electromagnetic parameters were used to obtain the setting time. Theoretical analysis and a setting time experiment verified the relationship between the selected parameters and the dielectric constant of the cement paste. Errors were reduced from 10.7% to 4.25%.**

***Index Terms*— Bandwidth, cement paste, patch antenna, resonant frequency, return loss, setting time, structural health monitoring.**

I. Introduction

CONCRETE structures are widely used worldwide [1], [2]. Cement setting time is one of the most important parameters during the construction of concrete structures [3], [4], [5]. Timing the cement setting period by the standard Vicat apparatus (VA) has been reported to have problems due to the need for continuous tests and experienced workers [6], [7]. The automatic VA (AVA) is a possible way to solve the problem [8]. However, the price of one AVA is much higher (over $3000 for the Humboldt Automatic, not including accessories), which is unsuitable for utilization in actual conditions. And the penetration-based detection method needs to insert a needle into the specimen to obtain the penetration resistance [9], which can cause minor damage to the unhardened concrete and visual offense [10]. Other possible methods listed in Table I also have similar problems. These conditions create a disqualified setting time unfit for construction [10], [11], [12], [13], [14], [15], [16], [17], [18], [19]. Considering the potential risk of corrosion, short-circuit, and open-circuit, the power system should be redesigned when cables are embedded inside the concrete. An automatic, wireless detection method is needed for a better observation.

TABLE I
EXISTED SETTING TIME DETECTION METHOD

Factor	Wire	Testing	Price	Ref.
Puncture strength	/	Manual, contacting, need specimen	$30	11-13
Puncture strength	Need	Automatic, contact, need specimen	$3,000	8, 14
Heat amount	Need	Automatic, in-site, insert node	Unsold	15
Humidity-Conductivity	Need	Automatic, non-contacting, in-site, insert node	Unsold	10, 16-18
Ultrasonic velocity	Need	Automatic, non-contacting, in-site, insert node	Unsold	19-21

To solve the abovementioned problem, the authors proposed several patch antenna sensors, expected to sense the setting time of cement passively and wirelessly [22], [23]. The resonant frequency shifts can reflect the moisture content change during the cement hydration and consequently determine the setting time of the cement. And an radio frequency identification (RFID) reader can interrogate the resonant frequency of the patch antenna wirelessly without a power supply on the node. However, the patch's resonant frequency depends not only on the moisture content of the covering material but also on other environmental impacts. This influence is even larger when the detection of backscattering wave is needed for the wireless interrogation. One of the most traditional and effective way to get rid of environmental impacts is decouple the influence by multiparameters [24], [25]. Using multiparameters to detect the setting time together is expected to show a potential dealing with environmental effects by decoupling the influence of each environmental parameter (e.g., temperature, humidity), while the effectiveness of the multiparameters for setting time detection is still unknown.

Manuscript received 29 June 2023; revised 17 August 2023; accepted 6 September 2023. Date of publication 20 September 2023; date of current version 17 October 2023. This work was supported in part by the National Natural Science Foundation of China under Grant 52178298 and Grant 52078375 and in part by the Top Discipline Plan of Shanghai Universities–Class I. The Associate Editor coordinating the review process was Dr. Zhengyu Peng. *(Corresponding author: Liyu Xie.)*

Zhuoran Yi and Liyu Xie are with the Department of Disaster Mitigation for Structures, Tongji University, Shanghai 200092, China (e-mail: linsmyk@gmail.com; liyuxie@tongji.edu.cn).

Songtao Xue is with the Department of Disaster Mitigation for Structures, Tongji University, Shanghai 200092, China, and also with the Department of Architecture, Tohoku Institute of Technology, Sendai 982-8577, Japan (e-mail: xue@tongji.edu.cn).

Guochun Wan is with the Department of Electronic Science and Technology, Tongji University, Shanghai 200092, China (e-mail: wanguochun@tongji.edu.cn).

Chunfeng Wan is with the Key Laboratory of Concrete and Prestressed Concrete Structure, Ministry of Education, Southeast University, Nanjing 210096, China (e-mail: wan@seu.edu.cn).

Digital Object Identifier 10.1109/TIM.2023.3317380

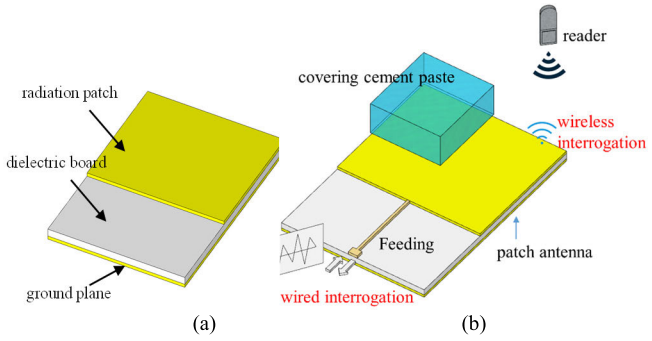

Fig. 1. Concept figure of patch antenna. (a) Model of typical patch antenna. (b) Test setup.

This article evaluates the effectiveness and workability of a patch antenna's multiparameters for detecting the cement hydration setting time, namely the patch antenna's resonant frequency, radiation efficiency, and bandwidth. The moisture content of the covering material will influence the impedance matching of the antenna sensor, causing a shift in bandwidth and radiation efficiency. Based on this relationship, the extra two parameters are expected to achieve the setting time detection in a different root other than using the resonant frequency of the patch antenna. The authors used theoretical analysis and simulation to analyze the radiation efficiency and bandwidth of a regular rectangular patch antenna, which proved to have a nearly linear relationship with the dielectric constant change of the covering material. Then, the other two parameters were utilized to detect the setting time of the cement, as well as the resonant frequency. Since a vector network analyzer (VNA) was utilized to interrogate the proposed patch antenna, the return loss was used instead of radiation efficiency. The initial and final setting times are then obtained from the peak value of the change rate of above three parameters separately.

This article is arranged as follows. Section II calculates the fundamental relationship between the antenna characteristic (resonant frequency, return loss, and bandwidth) and the dielectric constant of the upper material. This relationship is further confirmed by simulation in an Ansoft high-frequency structure simulator (Ansoft HFSS) in Section III. An experiment is then carried out, which was designed to measure cement's setting time and to check the workability of the three utilized parameters. Conclusions are then drawn, and future research potential is discussed.

II. Methodology

To detect the setting time, the resonant frequency, return loss, and bandwidth are examined based on their linear relationship with the change in moisture content of the top layer of cement. In this section, the ties between the cement setting and moisture content are first clarified by defining the mechanics behind the hydration principle of cement. Then, the dielectric constant of the top cement layer is tested to prove its linear relationship with the moisture content according to the homogeneous medium assumption. The final step is to analyze the effects of the changes in the dielectric constant in this upper layer of cement based on the three selected parameters.

A. Relationship Between Moisture Change and Setting Time

The very early stage of cement hydration can be divided into four parts: the initial reaction period, induction period, acceleration period, and post-acceleration period. The initial setting happens at the end of the induction period. Based on the previous research [22], the initial setting time can be directly obtained from when the moisture content first changes rapidly. The final setting time is assumed to happen in the medium of the acceleration period. The hydration speed of the final setting time is assumed to be a peak, as described in (1). The setting time of cement paste can be obtained from the change rate of the moisture content

$$g(t_{\text{fin}}) > g(t_{\text{fin}} \pm \Delta t), \quad \Delta t \in R \tag{1}$$

where t_{fin} is the final setting time and Δt is the time step. $g(t_{\text{fin}})$ is the change rate of moisture content, which is equal to the differential coefficient of the moisture content $f(t)$, as defined in the following equation:

$$g(t) = f'(t). \tag{2}$$

B. Moisture Change During Cement Hydration

In the very early age of hydration, cement can be regarded as a homogeneous material mixed with water, cement, and air [26]. The dielectric constant of the cement paste K can be regarded as the combination of the contents dielectric constant. Since the dielectric constants of cement and air are nearly the same compared with the dielectric constant of water, they are regarded as the same to simplify the calculation, described as follows [27]:

$$D^{0.5} = R_1 D_w^{0.5} + (R_2 + R_3) D_s^{0.5} \tag{3}$$

where R_1, R_2, and R_3 are the volume fraction of water, cement, and air. D_w, D_s, and D are the dielectric constant of water, cement, and mixed cement paste. The value of D_w and D_s is set as 82 and 4 based on previous research [28]. As presented in Yi et al. [22], [23], assuming the moisture content decreases from 25% to 10% during the very early hydration state, the change in the dielectric constant of cement paste is nearly linear based on (3). Hence, it is possible to monitor the moisture content by detecting the dielectric constant of cement paste.

C. Effects on Resonant Frequency, Return Loss, and Bandwidth

The radiation factor of a patch antenna can be selected to evaluate the average dielectric constant of nearby material. A typical rectangular patch antenna shown in Fig. 1(a) consists of a radiation patch, a dielectric board, and a ground plane. During the measurement, the patch antenna can be interrogated by the plane wave wirelessly or via the feed line, as shown in Fig. 1(b). Since this article mainly focuses on the performance test of the proposed sensing node and parameters, the wired interrogation system was selected as the test objective [29], [30]. The wireless interrogation will be the next step by measuring the radar cross section (RCS) curve instead of the S_{11} curve. The interrogation system will be renewed to deal

with complex environmental effects and lengthen the detection distance in the future.

The selected sensing parameters are radiation efficiency (replaced by return loss in this article), bandwidth, and resonant frequency. It should be noted that although the proposed three parameters can also be obtained from the RCS curve wirelessly, accurately detecting the proposed parameters will be a new important topic. In this section, the relationship between selected parameters and the dielectric constant of the patch antenna's upper material is calculated theoretically based on the radiation theory.

The first parameter is the resonant frequency. The resonant frequency f_0 of a typical rectangular patch antenna can be calculated by [31]

$$f_0 \approx c/2L_r\sqrt{\varepsilon_1} \tag{4}$$

where c is the light speed, ε_1 is the dielectric constant of the board, and L_r is the length of the patch antenna radiation patch. The covered cement mainly affects the resonant frequency by the fringe effect, which is considered in the following equation based on previous research [22], [23], (5), as shown at the bottom of the page, where ε_2 and ε_3 are the dielectric constant for the covered cement and air. q_{1n}, q_{2n}, and q_3 are the effect factor for the dielectric board, covered cement, and air. q_4 is the revised factor for the error caused by the assumption of an infinite air layer. Combining (4) and (5), the effects of the covered cement on the resonant frequency can be summarized as

$$f_0 \approx c/2L_r\sqrt{\varepsilon_e}. \tag{6}$$

The next parameter is bandwidth. The quantity factor mainly decides the bandwidth of a patch antenna. As mentioned in the research of Balanis [32], assuming the limit of the voltage standing wave ratio (VSWR) is ρ, the bandwidth BW within the range ρ is

$$\mathrm{BW} \approx \frac{\rho - 1}{Q_T\sqrt{\rho}} \tag{7}$$

where Q_T is the quantity factor calculated by

$$Q_T = \left[\frac{120\lambda h_1 G_r}{\varepsilon_e ab(1 - 3.4H_e)} + \frac{\delta_{\mathrm{skin}}}{h_1} + \tan\delta\right]^{-1} \tag{8}$$

where λ is the wavelength of the patch antenna. a and b are the length and width of the patch antenna. δ and δ_{skin} are the patch antenna's loss tangent angle and skin depth. H_e and G_r are constant values.

Based on Yang et al.'s research, the effective width, W_{ef}, and dielectric constant, ε_e, of the patch antenna will increase when covered by dielectric material with a dielectric constant higher than the dielectric board. Hence, the effect of covering cement on the bandwidth can be described as

$$\mathrm{BW} = F(\varepsilon_e, W_{\mathrm{ef}}). \tag{9}$$

Based on (9), the bandwidth will change with the dielectric constant and the width. According to Bahl et al. [33], the bandwidth will increase with the dielectric constant of the covering material. Hence, it can be used as a sensing parameter if the relationship is linear enough.

The final parameter is return loss. The return loss can be regarded as the representation of the antenna impedance matching, which can be calculated as

$$S_{11} = -20\log(1/|\Gamma|) \tag{10}$$

where Γ is the voltage reflection coefficient defined as

$$\Gamma = (Z_{\mathrm{in}} - Z_0)/(Z_{\mathrm{in}} + Z_0) \tag{11}$$

where Z_0 is the characteristic impedance defined by (12), nearly constant when the antenna parameter is decided. Z_{in} is the input impedance of the antenna. Equation (13) clarifies it by a function of the signal frequency f

$$Z_0 = \sqrt{L/C} = \frac{377}{\sqrt{\varepsilon_e}} \times \left[\frac{W_l}{h_l} + 1.393 + 0.667\ln\left(\frac{W_l}{h_l} + 1.444\right)\right]^{-1} \tag{12}$$

$$Z_{\mathrm{in}}(f) = R\Big/\left(1 + Q_T^2 m^2\right) - j\left[RQ_T m\Big/\left(1 + Q_T^2 m^2\right)\right] \tag{13}$$

where L and C are the equivalent inductance and capacitance of the antenna. W_l and h_l are the width and length of the feed line. m is a resonant factor defined by (14) R, which is the equivalent resistance calculated by (15) [32]

$$m = f/f_R - f_R/f \tag{14}$$

$$R \approx 60c/k_\varepsilon f_R \tag{15}$$

where f_R is the resonant frequency. f is the signal frequency. k_ε is the permittivity of free space. Since only the return loss in the resonant point is considered, the input resistance can be rewritten as

$$Z_{\mathrm{in}}(f_R) = R. \tag{16}$$

Hence, the influence on the return loss can be described as

$$S_{11}(f_e) = F(\varepsilon_e, W_{\mathrm{ef}}). \tag{17}$$

According to (17), the return loss is decided by the patch antenna's equivalent dielectric constant and width. Hence, the proposed three parameters are influenced by the covered material's dielectric constant.

D. Environmental Effect

Based on the theoretical calculation below, the resonant frequency, bandwidth, and return loss are all related to the dielectric constant of the covering material. Hence, all of them can detect the setting time of the covered cement paste. When the environmental effects are not considered, the detected setting time by these three factors should remain the same.

$$\varepsilon_e = \varepsilon_1 q_{1n} + \frac{\varepsilon_1(1 - q_{1n})^2 \times \left[\varepsilon_2^2 q_{2n} q_3 + \varepsilon_2\varepsilon_3(q_{2n}q_4 + (q_3 + q_4)^2)\right]}{\varepsilon_2^2 q_{2n} q_3 q_4 + \varepsilon_1(\varepsilon_2 q_3 + \varepsilon_3 q_4)(1 - q_{1n} - q_4)^2 + \varepsilon_2\varepsilon_3 q_4[q_{2n}q_4 + (q_3 + q_4)^2]} \tag{5}$$

TABLE II
INFLUENCE DEGREE OF ENVIRONMENTAL FACTOR

Factor	Resonant frequency	Bandwidth	Return loss
Temperature	◎	○	○
Inside bar (above)	◎	×	×
Inside bar (under)	×	◎	◎
EMI	×	○	◎
Crack distribution	◎	○	○

INFLUENCE: (◎>○>×)

However, when considering practical utilization, the environmental effects will also influence the selected three parameters. Except for the humidity of cement paste (the main factor), the main environmental factors are the inside bar, crack distribution, temperature, interrogation distance, and electromagnetic interference (EMI).

The inside bar will introduce an extra conductor layer to the embedded patch antenna. The bar above the patch antenna can be regarded as an additional resonant member and affects the resonant frequency [34], while highly influencing the return loss (radiation efficiency) by changing the impedance matching when under the patch antenna [35], [36]. The EMI and interrogation distance will mainly affect the return loss by decreasing the signal-to-noise ratio (SNR). The crack distribution will shift the bandwidth and return loss by increasing the loss factor of the concrete [37], [38]. The temperature is the most significant influence factor. On the one hand, it can considerably affect resonant frequency according to the expansion effect of the dielectric board. On the other hand, the drift effect to the dielectric constant of the dielectric board will influence the bandwidth, return loss, and resonant frequency. All of the effects are listed in Table II, and their effectiveness degree is measured by the following symbols, with ◎ having the greatest effect, followed by ○, which has a median effect, and × having the least effect.

Hence, though all the sensing parameters help detect the setting time according to the dielectric constant change of covered cement, the sensitivity to the environmental factors of all three parameters is different. Hence, it is possible to decrease the influence of the environmental factor by measuring these parameters together [39].

III. THEORY/CALCULATIONS

Based on the analysis in Section II, the dielectric constant of covered cement can be reflected by the resonant frequency, return loss, and bandwidth. The relationship is further calculated in this section to show the detailed relationship. The basic parameters of the calculated rectangular patch antenna are determined to simplify the calculation, as Tables III and IV shown. The equation proposed in Section II is first used for calculation. Then, a model in HFSS is established to verify the results.

A. Theoretical Calculation

Based on the equations mentioned in Section II, using the setting in Tables III and IV, the relationship between the antenna's parameters (resonant frequency, return loss, and bandwidth) and the dielectric constant of covered cement is shown in Fig. 2.

TABLE III
PARAMETERS OF UTILIZED PATCH ANTENNA SENSOR

Parameters	W	W_r	L	L_r	h
Value (mm)	51	49	48	41.3	0.508
Parameters	ε_r (1)	$tg\delta$			
Value	2.2	0.0009			

TABLE IV
PARAMETERS OF UTILIZED ENVIRONMENT

Parameters	h_2 (mm)	$\varepsilon_{2\text{-}min}$ (1)	$\varepsilon_{2\text{-}max}$(1)	ε_3 (1)
Value	10	7	13	1

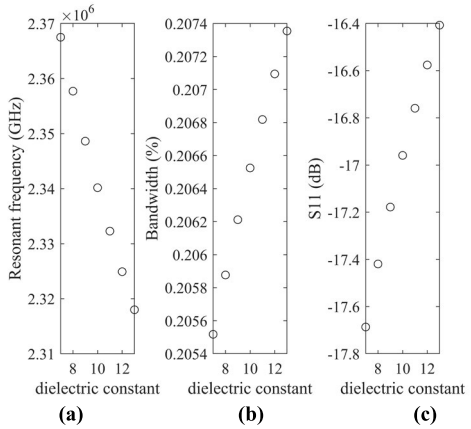

Fig. 2. Relationship between the antenna's parameters and dielectric constant of covering cement. (a) Resonant frequency. (b) Bandwidth. (c) Return loss (S_{11}).

When the height of the covering cement is kept at 30 mm, the resonant frequency, bandwidth, and return loss all have a nearly linear relationship based on the dielectric constant of the covering cement. These parameters can now obtain the setting time based on the selected factors.

B. Simulation

The numerical model plotted in Fig. 3 is established in an Ansoft high-frequency structure simulator 15 (HFSS 15) based on the parameters in Tables III and IV. A block with a changeable dielectric constant is set on a rectangular patch antenna. The dielectric board of the patch antenna is made of RT/duroid[1] 5880 laminates. The model is fed by the wave port at the end of the patch antenna. All models are embedded in an air box with a length of more than a quarter wavelength of the antenna to meet the needs of the simulator under far-field radiation.

Considering the condition with and without cement ($\varepsilon_2 = 7$) as a load, the radiation patterns ($\varphi = 90°$) at resonant frequency are simulated and further shown in Fig. 4. The

[1]Registered trademark.

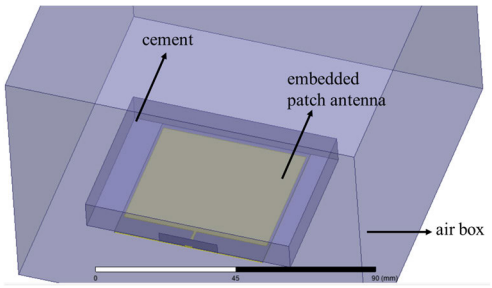

Fig. 3. Analysis model using HFSS 15.

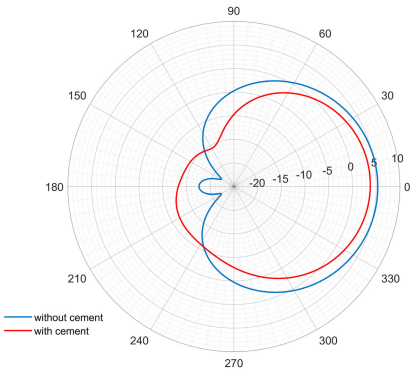

Fig. 4. Radiation pattern of patch antenna with and without cement load.

directivity is similar, while the maximum gain decreases from 5.32 to 3.75 when the cement load has been added.

The S_{11} curve of the patch antenna is then shown in Fig. 5. With the increase of the upper cement's dielectric constant, the patch antenna's resonant frequency decreased, but the bandwidth and the return loss increased.

Then the value of the resonant frequency, bandwidth, and return loss is calculated from the return loss curve and further plotted in Fig. 6. Due to the simplification of the model, the theoretical calculation shows a different value compared with the simulation. However, the linear trend of the selected three parameters is the same. Besides, the linear correlation coefficient for the resonant frequency and bandwidth is higher than 0.99, indicating excellent workability for the detection. The linearity for the results of return loss is not satisfactory. However, it continues to increase monotonically. Besides, the correlation coefficient achieves 0.95 when using quadratic function fitting, as shown in Fig. 6(d), which is also good enough for setting time detection.

IV. Experiment

An experiment is carried out to confirm the proposed sensing parameters' workability further, as shown in Fig. 7. The antenna sensor is fabricated based on the parameters listed in Tables III and IV. Three layers of waterproof film are covered on the antenna to eliminate the effects of contact with water. Then the fabricated antenna sensor is set inside an acrylic container. Cement paste with a mix proportion of 0.295 is fabricated and then directly put inside the container until the height of the cement achieves 30 mm. The measured condition is shown in Table V. A standard container is also

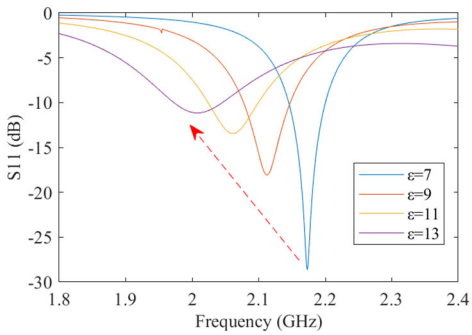

Fig. 5. Return loss curve of the model.

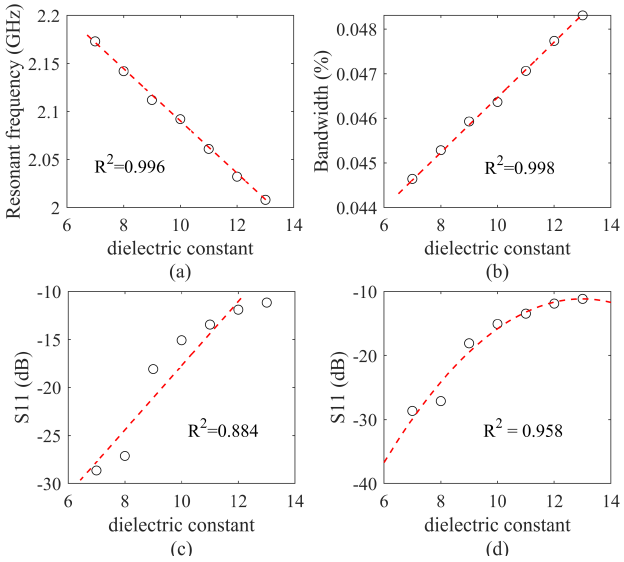

Fig. 6. Relationship between the antenna's parameters and dielectric constant of covering cement. (a) Resonant frequency. (b) Bandwidth. (c) Return loss, (S_{11})-linear. (d) Return loss (S_{11})-quadratic.

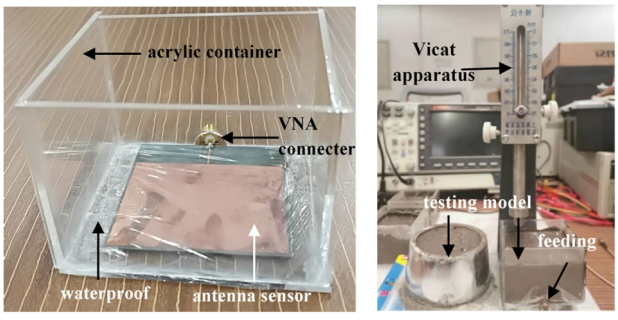

(a) (b)

Fig. 7. Sensing parameter experiment to confirm workability. (a) Test model. (b) Test setup.

filled for the standard testing of setting time by a VA. After that, the antenna sensor is interrogated by a VNA every 10 min until the cement achieves the final setting.

A. Results From VA

The depth of penetration and state are shown in Fig. 8. The initial setting time is obtained from the point when the penetration depth decreases to 68 mm. The final setting time is

TABLE V
PARAMETERS OF TESTING CEMENT BLOCK

Parameters	Dimension (mm^3)	Cement height (mm)	Temperature	Humidity
Value	52 x 73 x 60	30	20 °C	39%

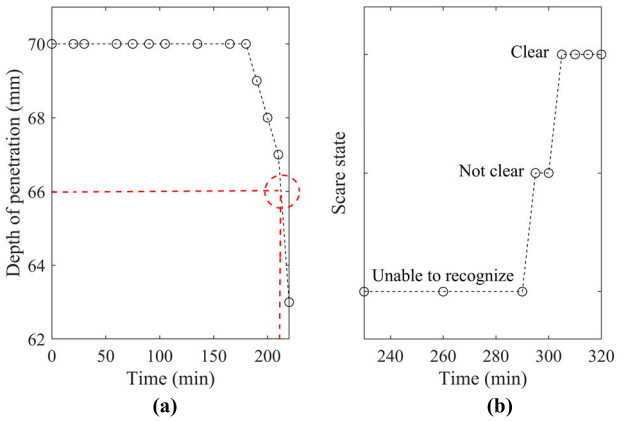

Fig. 8. Data of the VA testing. (a) Initial setting. (b) Final setting.

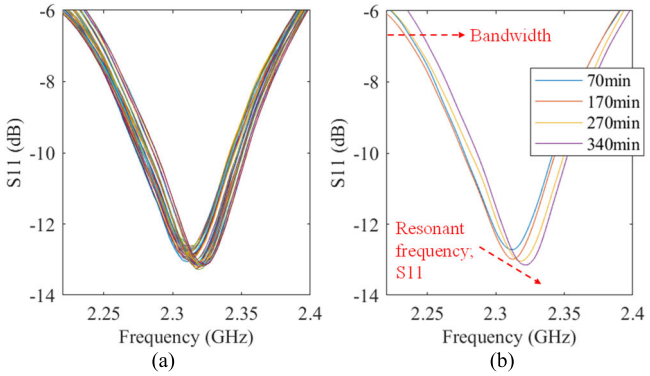

Fig. 9. Returned loss curve in the experiment. (a) Basic. (b) Selected example.

when the needle cannot produce a scar or mark on the surface of the cement.

From the measurement, the initial setting time is 215 min, and the final setting time is 305 min, respectively.

B. Results Using the Parameter Separately

All the measured return loss curves are shown in Fig. 9(a). Some of them at several different times are selected and further plotted in Fig. 9(b). With the increase of time, the resonant frequency and return loss tend to increase, and the bandwidth tend to decrease, which is fit with the prediction in the theoretical calculation and simulation in Section III.

Then the selected multiparameters are obtained from the return loss curve. Normalization is applied to the multiparameters to compare with each other more easily. After that, a moving window method mentioned by [20] and [21] is utilized to obtain the change rate. The slope of the fitting curve within the time range of $[t_i - \Delta t/2,\ t_i + \Delta t/2]$ is selected to be the change rate at time t_i, as shown in Fig. 10. It can be regarded as a smooth filtering for multiparameters results

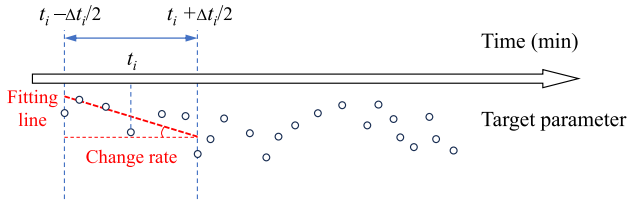

Fig. 10. Basic concept of the proposed moving window method.

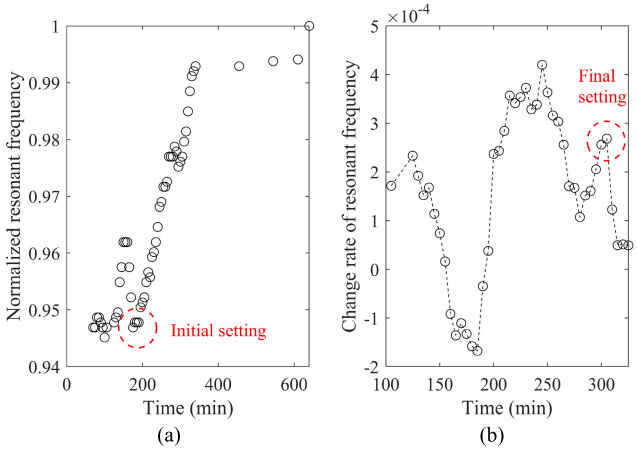

Fig. 11. Relationship between normalized resonant frequency and time. (a) Initial setting. (b) Final setting.

when the change rate is needed. The smooth factor Δt is set as 60 min (other settings of Δt, such as 40, 50, or 70 min, also work).

Based on the proposed method, the detected results using resonant frequency are shown in Fig. 11. As discussed in Section II-A, the time when the resonant frequency starts to increase rapidly is regarded as the initial setting, and the time when the change rate of the resonant frequency finally decreases is the final setting time. Due to the environmental influence or the measurement error, there may have multiple possible answers which can fit the requirement of the setting time judgment. Since the influence of hydration is hugest, the answer followed with the longest monotonous variation range will be selected as the correct answer. Besides, during the construction, the identified initial setting time should be no later, and the final setting time be no earlier compared with the exact setting time due to the requirement of pouring, pumping, or set up of scaffolding. Hence, if the following variation range is similar for several possible answers, the earlier initial setting and later final setting will be selected as the correct answer.

Based on this rule, according to the measured resonant frequency, the initial and final setting times were 190 and 305 min, respectively.

A method to the method using resonant frequency, another method is utilized to obtain the setting time according to the bandwidth and return loss data, as shown in Figs. 12 and 13, respectively. It should be noted that only the absolute value of the change rate has meaning. Since the bandwidth decreases with time increase, most of the change rate is negative. Hence, different from the resonant frequency and S_{11}, the final setting time will be selected when the change rate increases.

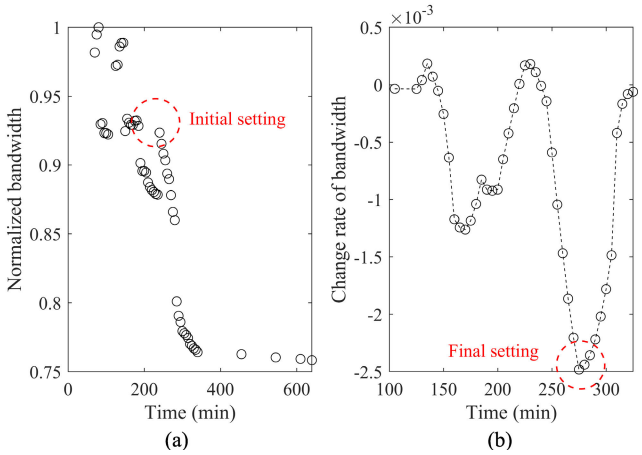

Fig. 12. Relationship between normalized bandwidth and time. (a) Initial setting. (b) Final setting.

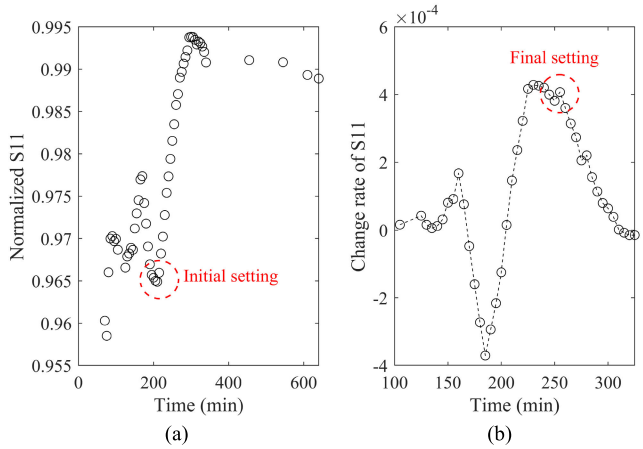

Fig. 13. Relationship between normalized S_{11} and time. (a) Initial setting.(b) Final setting.

C. Simple Data Fusion for Proposed Parameters

Since three datasets were used to obtain the initial and final setting time, it is possible to increase the measurement accuracy by evaluating a data fusion method. Two simple data fusion methods are considered here. The first one directly compares the detected setting time from the three parameters. Another utilized data fusion method combines the normalized three parameters calculated as

$$C = n_f - n_b/5 + n_s \tag{18}$$

where C is the combined data. Then, n_f, n_b, and n_s are the normalized resonant frequency, bandwidth, and return loss, respectively. Since the change range of the bandwidth is about five times greater than the other two parameters, the normalized bandwidth is divided by 5 to consider these three parameters equally. The combined data, C, and the change rate of C are then utilized to get the initial and final setting, as shown in Fig. 14.

The results are compared with each other in Table VI and Fig. 15. The search for errors comes from the following possibilities.

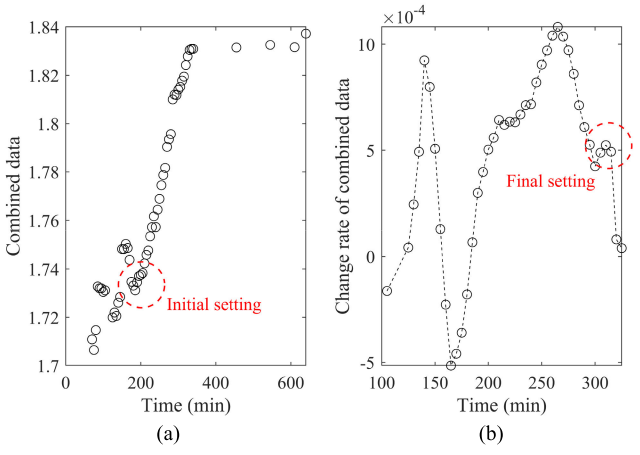

Fig. 14. Relationship between combined data and time. (a) Initial setting. (b) Final setting.

TABLE VI
ERROR OF THE SETTING-TIME DETECTION OF CEMENT PASTE

Parameters	Initial setting (min)	Error (%)	Final setting (min)	Error (%)	Average error (%)
Vicat apparatus	215	/	305	/	/
f	190	11.6	305	0	5.8
BW	240	11.6	275	9.8	10.7
$S11$	210	2.3	255	16.4	9.4
Combined data	200	6.9	310	1.6	4.25
Simple average	213.3	0.7	278.3	8.8	4.75

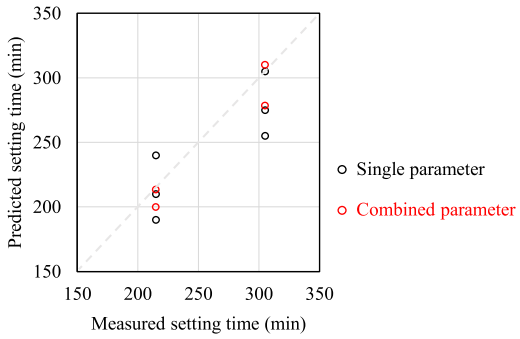

Fig. 15. Prediction of setting time.

1) System Error: The proposed three parameters' errors are highly familiar, so the system error is first considered. The hydration period of the cement inside the standard container and the acrylic container may be slightly different, causing errors in the setting determination.

2) Environmental Influence: The change in the temperature and humidity of the environment can also affect the final detected results.

From Fig. 15, the prediction tends to underestimate the setting time, which is safe for the initial setting but dangerous for the final setting. However, since the error using the proposed sensing parameters is all within 17% separately, the influence of underestimation is not severe. One adjusting parameter can be set in the future to make the final setting prediction safer.

After the simple average, the average maximum mistake decreased from 10.7% to 4.75%. This error is further reduced to 4.25% when considering combined data. That is, the proposed simple data fusion methods can increase measurement accuracy compared with the worst condition obtained by the multiparameters. Since the exact setting time cannot be obtained in real conditions, the proposed data fusion method can increase the robustness of the measurement.

Besides, due to the selection method proposed in Section IV-B, compared with the average results, the proposed simple data fusion tends to get the initial setting time with the hugest variation range, and the final setting time with the largest value. Hence, the error trend is inconsistent between the proposed simple data fusion and average results. The utilized methods only show a possible way to obtain better results by data fusion. Since the multiparameters have been verified to be effective for setting time detection, a better data fusion method using proposed multiparameters is expected to be proposed to deal with the possible environmental noise in the future. After that, the wireless detection method is planned to be analyzed.

V. Conclusion

This article introduced three parameters (resonant frequency, return loss, and bandwidth) of the patch antenna sensor to detect cement setting time. An equivalent model based on conformal mapping theory was proposed to verify the workability of the proposed sensing parameters. Then an HFSS model, version 15, was established to check the results further. Next, the patch antenna sensor was fabricated, and experiments were conducted to test the sensor in the laboratory. The error for setting time prediction was within 17% for each parameter separately, and the average error was smaller than 11%, indicating all the parameters are effective for setting time detection. This error can be decreased by 5% after considering the simple data fusion methods. Since the environmental disturbances are different for the proposed three parameters, this sensor is expected to reduce the environmental effects by measuring these parameters together.

References

[1] J. B. Pereira and G. F. Maciel, "Automated slump test: An effective alternative in predicting rheological properties and an efficient tool for providing the quality control of materials," *Measurement*, vol. 178, Jun. 2021, Art. no. 109384.

[2] N. Yang, Y. Lei, J. Li, H. Hao, and J.-S. Huang, "A substructural and wavelet multiresolution approach for identifying time-varying physical parameters by partial measurements," *J. Sound Vib.*, vol. 523, Apr. 2022, Art. no. 116737.

[3] S. Xue, X. Li, L. Xie, Z. Yi, and G. Wan, "A bolt loosening detection method based on patch antenna with overlapping sub-patch," *Struct. Health Monitor.*, vol. 21, no. 5, pp. 2231–2243, Sep. 2022.

[4] K. Jiang, L. Xie, S. Xue, and G. Wan, "Capacitively-coupled dual ring antennas for bolt loosening detection," *Measurement*, vol. 200, Jan. 2022, Art. no. 111605.

[5] D. Lootens and D. P. Bentz, "On the relation of setting and early-age strength development to porosity and hydration in cement-based materials," *Cement Concrete Compos.*, vol. 68, pp. 9–14, Apr. 2016.

[6] Standards Press of China. *General Administration of Quality Supervision, Inspection and Quarantine (AQSIQ) and Standardization Administration (SAC) of the People's Republic of China. GB/T 1346-2011 Test Methods for Water Requirement of Normal Consistency, Setting Time and Soundness of the Portland Cement, National Standard of the People's Republic of China*. Accessed: Oct. 2021. [Online]. Available: https://www.chinesestandard.net/PDF.aspx/GBT1346-2011

[7] L. Xie, Z. Xia, S. Xue, and X. Fu, "Detection of setting time during cement hydration using ground penetrating radar," *J. Building Eng.*, vol. 60, Nov. 2022, Art. no. 105166.

[8] G. Berger, C. Ullner, G. Neumann, and H. Marx, "New characterization of setting times of alkali containing calcium phosphate cements by using an automatically working device according to gillmore needle test," *Key Eng. Mater.*, vols. 309–311, pp. 825–828, May 2006.

[9] *Standard for Test Method of Performance on Ordinary Fresh Concrete*, Standard GB/T50080-2002, 2007.

[10] K. J. Akram, A. Ahmed, and T. Islam, "Fringing field impedance sensor for hydration monitoring and setting time determination of concrete material," *IEEE Trans. Instrum. Meas.*, vol. 69, no. 5, pp. 2131–2138, May 2020.

[11] X. Kang, H. Lei, and Z. Xia, "A comparative study of modified fall cone method and semi-adiabatic calorimetry for measurement of setting time of cement based materials," *Construct. Building Mater.*, vol. 248, Jul. 2020, Art. no. 118634.

[12] F. Li and J. Liu, "An experimental investigation of hydration mechanism of cement with silicane," *Construct. Building Mater.*, vol. 166, pp. 684–693, Mar. 2018.

[13] R. Ylmén, U. Jäglid, B.-M. Steenari, and I. Panas, "Early hydration and setting of Portland cement monitored by IR, SEM and Vicat techniques," *Cement Concrete Res.*, vol. 39, no. 5, pp. 433–439, May 2009.

[14] D. Jansen, J. Neubauer, F. Goetz-Neunhoeffer, R. Haerzschel, and W.-D. Hergeth, "Change in reaction kinetics of a Portland cement caused by a superplasticizer—Calculation of heat flow curves from XRD data," *Cement Concrete Res.*, vol. 42, no. 2, pp. 327–332, Feb. 2012.

[15] D. Luo, Z. Ismail, and Z. Ibrahim, "Added advantages in using a fiber Bragg grating sensor in the determination of early age setting time for cement pastes," *Measurement*, vol. 46, no. 10, pp. 4313–4320, Dec. 2013.

[16] J. Zhu, Y.-T. Tsai, and S.-H. Kee, "Monitoring early age property of cement and concrete using piezoceramic bender elements," *Smart Mater. Struct.*, vol. 20, no. 11, Nov. 2011, Art. no. 115014.

[17] C. Despas et al., "High-frequency impedance measurement as a relevant tool for monitoring the apatitic cement setting reaction," *Acta Biomaterialia*, vol. 10, no. 2, pp. 940–950, Feb. 2014.

[18] K. J. Akram, A. Ahmed, B. George, and T. Islam, "Evaluation of a cross-conductance sensor for cement paste hydration monitoring and setting time measurement," *IEEE Sensors J.*, vol. 23, no. 2, pp. 1584–1591, Jan. 2023.

[19] A. Smith, T. Chotard, N. Gimet-Breart, and D. Fargeot, "Correlation between hydration mechanism and ultrasonic measurements in an aluminous cement: Effect of setting time and temperature on the early hydration," *J. Eur. Ceram. Soc.*, vol. 22, no. 12, pp. 1947–1958, Nov. 2002.

[20] G. Trtnik, G. Turk, F. Kavčič, and V. B. Bosiljkov, "Possibilities of using the ultrasonic wave transmission method to estimate initial setting time of cement paste," *Cement Concrete Res.*, vol. 38, no. 11, pp. 1336–1342, Nov. 2008.

[21] J. Carette and S. Staquet, "Monitoring the setting process of mortars by ultrasonic P and S-wave transmission velocity measurement," *Construct. Building Mater.*, vol. 94, pp. 196–208, Sep. 2015.

[22] Z. Yi, S. Xue, L. Xie, and G. Wan, "Detection of setting time in cement hydration using patch antenna sensor," *Struct. Control Health Monitor.*, vol. 29, no. 1, pp. 1–10, Jan. 2022.

[23] Z. Yi, S. Xue, L. Xie, G. Wan, and C. Wan, "A slotted-patch antenna sensor with higher sensitivity for detecting setting time of cement paste," *IEEE Trans. Instrum. Meas.*, vol. 71, pp. 1–13, 2022.

[24] Y. Romero, R. M. A. Velásquez, and J. Noel, "Development of a multiple regression model to calibrate a low-cost sensor considering reference measurements and meteorological parameters," *Environ. Monitor. Assessment*, vol. 192, no. 8, pp. 1–11, Aug. 2020.

[25] S. Turrisi, A. Cigada, and E. Zappa, "A cointegration-based approach for automatic anomalies detection in large-scale structures," *Mech. Syst. Signal Process.*, vol. 166, Mar. 2022, Art. no. 108483.

[26] F. W. Taylor, *Cement Chemistry*, 2nd ed. London, U.K.: Thomas Telford Publishing, 1997.

[27] X. Zhang, X. Z. Ding, C. K. Ong, B. T. G. Tan, and J. Yang, "Dielectric and electrical properties of ordinary Portland cement and slag cement in the early hydration period," *J. Mater. Sci.*, vol. 31, no. 5, pp. 1345–1352, Mar. 1996.

[28] Z. J. Sun, "Estimating volume fraction of bound water in Portland cement concrete during hydration based on dielectric constant measurement," *Mag. Concrete Res.*, vol. 60, no. 3, pp. 205–210, Apr. 2008.

[29] R. Kozak, K. Khorsand, T. Zarifi, K. Golovin, and M. H. Zarifi, "Patch antenna sensor for wireless ice and frost detection," *Sci. Rep.*, vol. 11, no. 1, pp. 1–11, Jul. 2021.
[30] T. V. Padmavathy, D. S. Bhargava, P. Venkatesh, and N. Sivakumar, "Retraction note: Design and development of microstrip patch antenna with circular and rectangular slot for structural health monitoring," *Pers. Ubiquitous Comput.*, vol. 22, no. 5, pp. 883–893, Aug. 2023.
[31] S. Xue, Z. Yi, L. Xie, G. Wan, and T. Ding, "A passive wireless crack sensor based on patch antenna with overlapping sub-patch," *Sensors*, vol. 19, no. 19, p. 4327, Oct. 2019.
[32] C. A. Balanis, *Antenna Theory: Analysis and Design*, 4th ed. London, U.K.: Wiley, 2016.
[33] I. Bahl, P. Bhartia, and S. Stuchly, "Design of microstrip antennas covered with a dielectric layer," in *Proc. Antennas Propag. Soc. Int. Symp.*, vol. 18, Mar. 1980, pp. 589–592.
[34] S. Xue, Z. Yi, L. Xie, and G. Wan, "Double-frequency passive deformation sensor based on two-layer patch antenna," *Smart. Struct. Syst.*, vol. 6, no. 27, pp. 969–982, 2021.
[35] L. Ukkonen, L. Sydanheimo, and M. Kivikoski, "Effects of metallic plate size on the performance of microstrip patch-type tag antennas for passive RFID," *IEEE Antennas Wireless Propag. Lett.*, vol. 4, pp. 410–413, 2005.
[36] L. Sydänheimo, L. Ukkonen, and M. Kivikoski, "Effects of size and shape of metallic objects on performance of passive radio frequency identification," *Int. J. Adv. Manuf. Technol.*, vol. 30, nos. 9–10, pp. 897–905, Oct. 2006.
[37] J.-L. Liu, J.-Y. Xu, S. Lu, and H. Chen, "Investigation on dielectric properties and microwave heating efficiencies of various concrete pavements during microwave deicing," *Construct. Building Mater.*, vol. 225, pp. 55–66, Nov. 2019.
[38] Y. Chen, Y. Wen, and P. Li, "Characterization of PZT ceramic transducer embedded in concrete," *Sens. Actuators A, Phys.*, vol. 128, no. 1, pp. 116–124, Mar. 2006.
[39] F. M. Tchafa and H. Huang, "Microstrip patch antenna for simultaneous strain and temperature sensing," *Smart Mater. Struct.*, vol. 27, no. 6, Jun. 2018, Art. no. 065019.

Zhuoran Yi received the B.S. and M.S. degrees in civil engineering from Tongji University, Shanghai, China, in 2018 and 2021, respectively.

His current research interests include the smart sensors for the structural health monitoring and FMCW-based radio frequency identification (RFID) detection systems.

Songtao Xue received the B.S. degree in mechanics engineering from Tongji University, Shanghai, China, in 1985, and the M.S. and Ph.D. degrees in structural engineering from Tohoku University, Sendai, Japan, in 1989 and 1991, respectively.

From 1991, he was as an Assistant Professor with the Department of Architecture, Tohoku University, and then promoted to an Associate Professor, in 1995. Since 1996, he has been with Tongji University, where he is a Full Professor. In 2010, he joined the Department of Architecture, Tohoku Institute of Technology, Sendai, where he is currently the Director with the Department of Architecture. His research interests include structural health monitoring, seismic engineering, and structural vibration control.

Liyu Xie (Member, IEEE) received the B.S. and M.S. degrees in mechanics engineering from Tongji University, Shanghai, China, in 2000 and 2003, respectively, and the Ph.D. degree in system design engineering from Keio University, Tokyo, Japan, in 2009.

Since 2009, he has been with the College of Civil Engineering, Tongji University, where he is currently an Associate Professor. His current research interests include smart sensors, structural health monitoring, and structural vibration control.

Guochun Wan (Member, IEEE) received the M.S. and Ph.D. degrees in transportation information engineering and control from Tongji University, Shanghai, China, in 2005 and 2011, respectively.

In 2002, he became an Associate Professor with Tongji University, where he joined with the Department of Electronic Science and Technology, in 2006. His current research interests include signal and information processing, with an emphasis on error-correcting coding, VLSI architectures, radio frequency identification (RFID) strain sensor, and system-on-chip (SoC) design for communications, and coding theory applications.

Chunfeng Wan received the B.S. degree from the University of Electronic Science and Technology of China, Chengdu, China, in 1997, and the M.S. degree from Tongji University, Shanghai, China, in 2001, and the Ph.D. degree in system design engineering from Keio University, Tokyo, Japan, in 2009.

Since 2009, he has been with the School of Civil Engineering, Southeast University, Nanjing, China, where he is currently an Associate Professor. His current research interests include structural health monitoring and smart maintenance for civil infrastructures.